8th International Congress of Serbian Society of Mechanics
Kragujevac, Serbia, June 28-30, 2021

H_∞ PROPORTIONAL-INTEGRAL CONTROL OF A TURBOFAN ENGINE

Nemanja D. Zorić[1], Vladimir M. Jazarević[2], Aleksandar M. Obradović[1]

[1] Faculty of Mechanical Engineering,
The University of Belgrade, Kraljice Marije 16, 11120 Belgrade 35, Serbia
e-mail: nzoric@mas.bg.ac.rs, aobradovic@mas.bg.ac.rs
[2] Mechatronics Unmanned Systems & Technology Solutions d.o.o., Marka Oreškovića 1, Belgrade, Serbia
e-mail: vladimir.jazarevic@mustsolution.com

Abstract:

This paper presents the design of a thrust controller for a single-shaft turbofan engine at the operation point defined with following parameters: altitude = 0, Mach number = 0, angle of attack = 0. In that case, the dynamics of the engine depends only of the shaft angular velocity. Mathematical model for controller synthesis is obtained by solution of the set of nonlinear equations. Due to complexity of the engine, parameter uncertainties and exposure to various disturbances during exploitation, the H_∞ methodology for controller synthesis is applied. Since H_∞ based controller presents linear controller, it requires linear model of the plant for synthesis. Due to that, the plant needs to be linearized. From nonlinear simulation, the 1st order transfer functions can be obtained for selected intervals of shaft angular velocities. For controller synthesis, the fuel supply system is also included as the 1st order transfer function. Since obtained controllers present higher order controllers which may not be feasible for a real-time implementation because of hardware limitations, they are reduced to proportional-integral (PI) controllers by using the balanced reduction. Obtained controllers are then combined via gain-scheduling approach and simulation is performed.

Key words: Turbofan engine, H_∞ control, Proportional-integral control, Gain scheduling.

1. Introduction

Turbofan engine presents a nonlinear system with parameters varying during flight. It must provide a wide range of predictable and repeatable thrust performance over the entire operating envelope of the engine, which can cover the altitude from sea level to tens of thousands meters. Due to demand for precise thrust control, a turbofan engine must be operated by means of feedback control. The design of controllers capable of delivering this objective represents a challenging problem, since it presents the nonlinear system which parameters depends on operation points (shaft angular velocity, altitude, Mach number, angle of attack).

This paper presents the design of a thrust controller for a single-shaft turbofan engine at the operation point defined with following parameters: altitude = 0, Mach number = 0, angle of attack = 0. In that case, the dynamics of the engine depends only of the shaft angular velocity. Due to complexity of the engine, parameter uncertainties and exposure to various disturbances during exploitation, the robust control approach will be used for controller design, particularly H_∞ control methodology [1, 2]. The mathematical model for controller synthesis consists of nonlinear differential equations, maps, and tables which describe the dynamic and thermodynamic relationships of individual components of the engine such as inlet, fan, compressor, combustor, turbine and nozzle [3, 4]. This set of equation is numerically solved by using the Newton-Raphson method [5]. Since, H_∞ based controller presents linear controller, it requires linear model of the plant for synthesis. Due to that, the plant needs to be linearized. From nonlinear simulation, the 1st order transfer functions can be obtained for selected intervals of shaft angular velocities. For controller synthesis, the fuel supply system is also included as the 1st order transfer function. Since obtained controllers present higher order controllers which may not be feasible for a real-time implementation because of hardware limitations [6, 7, 8], they are reduced to PI controllers by using the balanced reduction [2]. Obtained controllers are then combined via gain-scheduling approach and simulation is performed.

2. Dynamic modeling of the turbofan engine

Turbofan engine can be represented as a single-input-single-output (SISO) system where the fuel mass flow rate is the input variable while the thrust is the output variable. In real cases (flight condition), the thrust cannot be measured directly, hence some other engine variable can be measured and, according this variable, the thrust can be estimated. The most appropriate variable is the shaft angular velocity since it can be easily measured. In this paper, the operation point defined with following parameters: altitude = 0, Mach number = 0, angle of attack = 0 is considered. The design point shaft angular velocity is $N_{\mathrm{dp}} = 36000\ \mathrm{rpm}$. Static relationships, obtained by solving nonlinear differential equations [3, 4], between the thrust, the shaft angular velocity and the fuel mass flow rate are presented in Fig. 1. Relationships, shown in Fig. 1, are presented for shaft angular velocities in range from 18000 rpm (which presents minimum shaft angular velocity) to 37800 rpm.

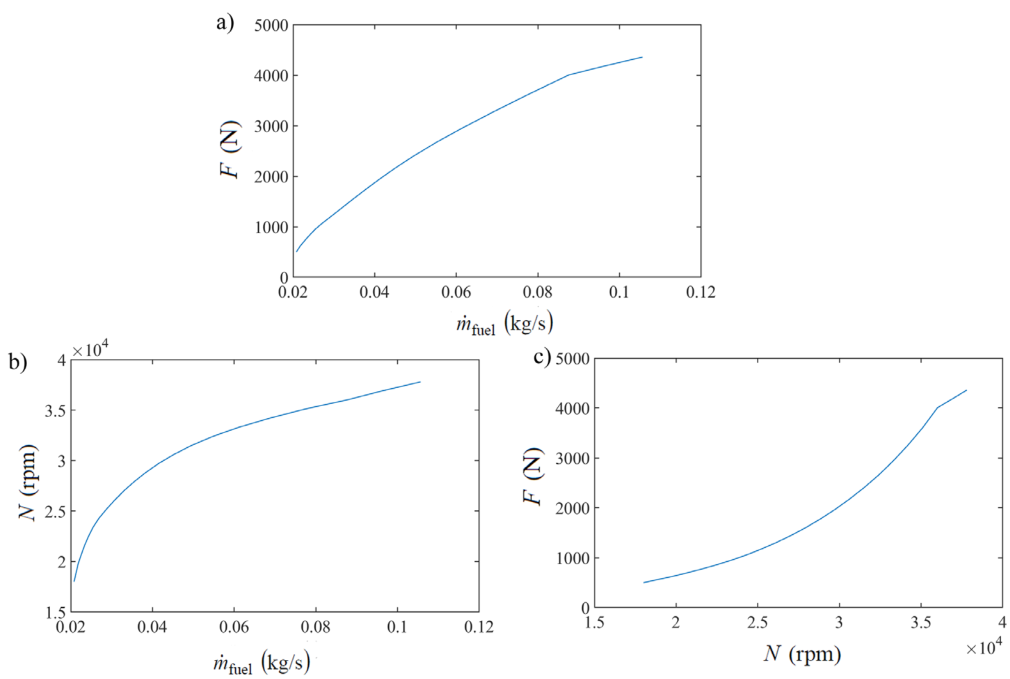

Fig. 1. Static plots: a) thrust versus fuel mass flow, b) shaft angular velocity versus fuel mass flow rate, c) thrust versus shaft angular velocity.

After that, the shaft angular velocities as well as the fuel mass flow rate are scaled on following way

$$\overline{N}_{\text{rel}} = \frac{N - N_{\min}}{N_{\text{dp}}}, \quad \overline{m}_{\text{fuel}} = \dot{m}_{\text{fuel}} - \dot{m}_{\text{fuel}}\left(N_{\min}\right), \tag{1}$$

where $\dot{m}_{\text{fuel}}\left(N_{\min}\right) = 0.020783\,\text{kg/s}$ presents the fuel mass flow rate which corresponds to the minimum shaft angular velocity. Static plots of obtained relative values are presented in Fig. 2.

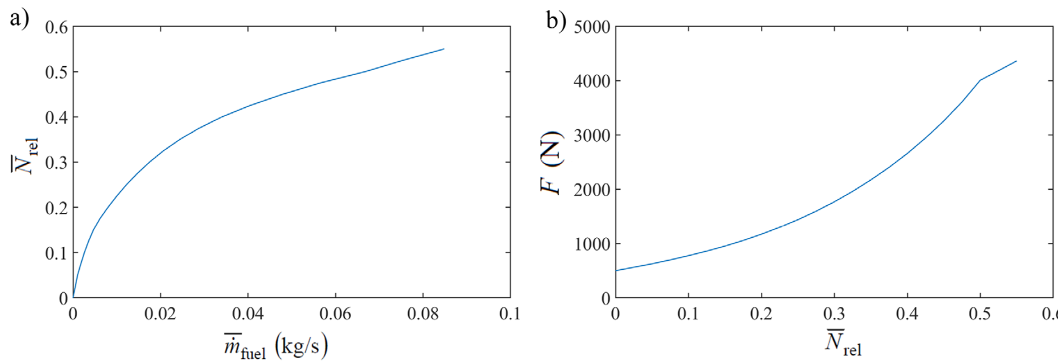

Fig. 2. Static plots: a) shaft relative angular velocity versus relative fuel mass flow rate, c) thrust versus shaft relative angular velocity.

During transient conditions, the shaft angular acceleration can be calculated as follows [4]

$$\dot{N} = \frac{1}{JN}\left(P_{\text{t}} - P_{\text{c}} - P_{\text{t\_loss}}\right), \tag{2}$$

where J presents the turbine inertia moment, while P_{t}, P_{c} and $P_{\text{t\_loss}}$ are the turbine power, the compressor power and the turbine power loss respectively. It can be concluded that the equation (2) presents the 1st order differential equation which right side depends on operation points and the fuel mass flow rate. In this case, since is single operation condition is considered, the right side depends only of the fuel mass flow rate. Thus, the relation between the shaft relative angular velocity and the relative fuel mass flow rate is:

$$\overline{N}_{\text{rel}} = \frac{G}{\tau s + 1}\overline{m}_{\text{fuel}} + C_0, \tag{3}$$

where G presents the static gain, while τ presents the time constant. The input/output of the previous equation can be written as

$$\Delta\overline{N}_{\text{rel}} = \frac{G}{\tau s + 1}\Delta\overline{m}_{\text{fuel}}, \tag{4}$$

so, the transfer function of the turbofan engine is

$$H_{\text{tf}}\left(s\right) = \frac{G}{\tau s + 1}. \tag{5}$$

In order to determine values of coefficients in equation (3), equation (2) is solved by using the transient simulation for step inputs of the fuel mass flow rate for following intervals of shaft relative angular velocities: 0-0.05, 0.05-0.075, 0.075-0.1, 0.1-0.125, 0.125-0.15, 0.15-0.175, 0.175-0.2, 0.2-0.225. 0.225-0.25, 0.25-0.275, 0.275-0.3, 0.3-0.325, 0.325-0.35, 0.35-0.375, 0.375-0.4, 0.4-0.425, 0.425-0.45, 0.45-0.475, 0.475-0.5, 0.5-0.525, 0.525-0.55. Obtained values are presented in Table 1. Fig. 3 presents the Bode plot of the turbofan engine model for each interval of shaft relative angular velocities.

$\overline{N}$	G	C_0	τ
0-0.05	48.8045	0	4.606172
0.05-0.075	33.0099	0.0162	2.360718
0.075-0.1	30.9424	0.0199	2.065262
0.1-0.125	26.1152	0.0324	1.774623
0.125-0.15	22.4592	0.0453	1.580028
0.15-0.175	16.9857	0.0708	1.133016
0.175-0.2	13.6049	0.0916	0.831947
0.2-0.225	12.3806	0.1013	0.706215
0.225-0.25	11.3295	0.1118	0.651042
0.25-0.275	9.9818	0.1283	0.584795
0.275-0.3	8.9672	0.1432	0.52687
0.3-0.325	7.8425	0.1628	0.467508
0.325-0.35	6.6627	0.1872	0.415282
0.35-0.375	5.7722	0.209	0.386997
0.375-0.4	4.7626	0.238	0.34638
0.4-0.425	3.9206	0.2667	0.297177
0.425-0.45	3.3241	0.2908	0.266099
0.45-0.475	2.906	0.3108	0.250627
0.475-0.5	2.4289	0.3377	0.225734
0.5-0.525	2.8969	0.3065	0.206143
0.525-0.55	2.6554	0.3247	0.194363

Table 1. Obtained values of coefficients in equation (3).

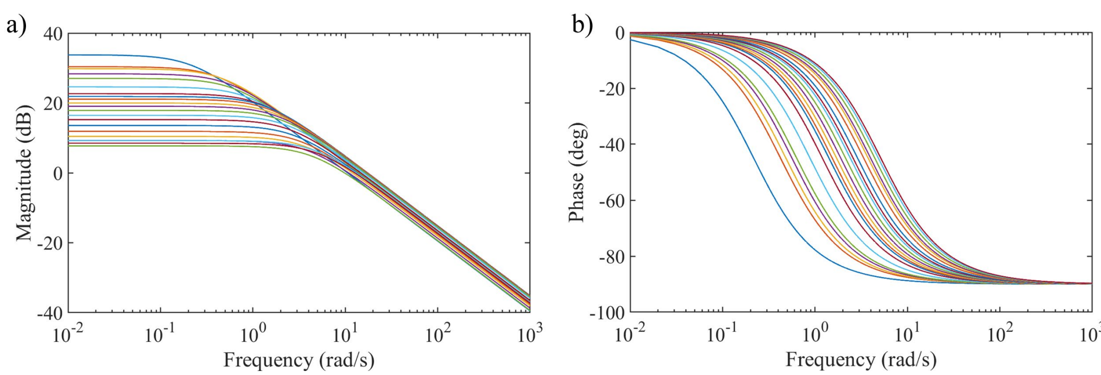

Fig. 3. Bode plot of the turbofan engine model: a) magnitude, b) phase.

For the fuel supply system, the geared pump is applied which can be modeled with the 1st order transfer function. In order to perform numerical simulation, the following transfer function is considered

$$H_{\text{fss}}(s) = \frac{1}{0.1s+1} . \tag{6}$$

Real value of the transfer function will be determined after experimental identification of the pump.

3. *H∞* control system design

A block diagram of the designed closed loop is presented in Fig. 4. The H_∞ controller is designed by using S/KS mixed-sensitivity approach [1]. Fig. 5 shows the standard mixed-sensitivity approach for reference tracking and control effort.

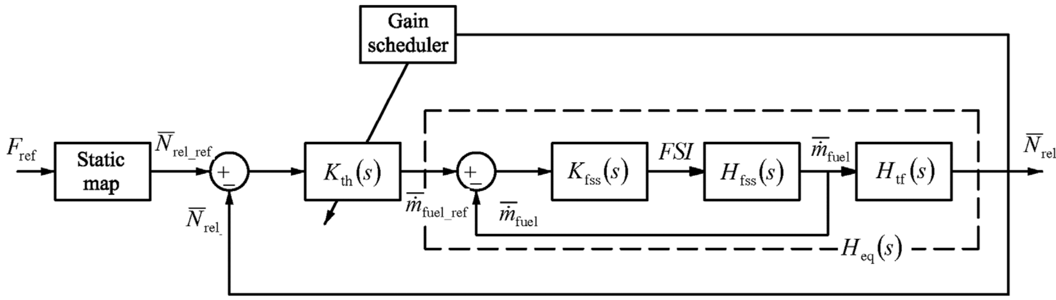

Fig. 4. Block diagram of the designed closed loop.

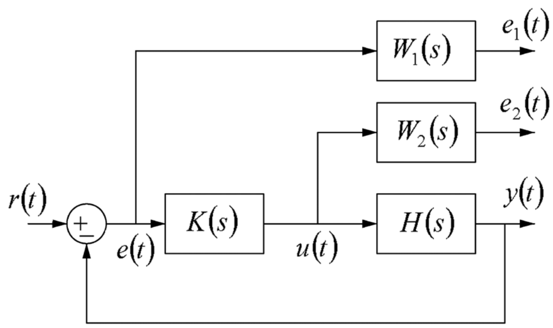

Fig. 5. S/KS mixed-sensitivity formulation.

The first stage is the fuel supply system controller ($K_{\text{fss}}(s)$) synthesis by setting the plant transfer function to be fuel supply system transfer function. After obtaining the fuel supply system controller, the second stage is the thrust controller ($K_{\text{th}}(s)$) synthesis where following equivalent transfer functions will be used:

$$H_{\text{eq}}(s) = H_{\text{tf}}(s)\frac{H_{\text{fss}}(s)K_{\text{fss}}(s)}{1+H_{\text{fss}}(s)K_{\text{fss}}(s)}. \tag{7}$$

3.1 Fuel supply controller design

For the fuel supply controller design, following weighting functions are selected:

$$W_1(s) = 0.5\frac{s+12}{s+0.012},\; W_2(s) = 0.5\frac{s+0.0001}{s+10}, \tag{8}$$

and the following 3rd order controller is obtained:

$$K_{\text{fss}}(s) = \frac{1067s^2+2.134\cdot 10^4 s+1.067\cdot 10^5}{s^3+1210s^2+1.202\cdot 10^4 s+144}. \tag{9}$$

After elimination of negligible states by using balanced reduction, the 3rd order fuel supply system controller can be reduced to the 1st order controller:

$$K_{\mathrm{fss}}(s)=\frac{0.8816s+8.89}{s+0.012}. \tag{10}$$

Since the second term in the denominator in the 1st order controller (0.012) is much smaller than the first term (1) it can be omitted, which finally leads to the PI controller:

$$K_{\mathrm{fss}}(s)=0.8816+\frac{8.89}{s}. \tag{11}$$

3.2 Thrust controller design

For obtaining thrust controllers, the PI fuel supply controller is considered in Equation (7). The Bode plot of equivalent plants (Equation (7)) is presented in Fig. 6.

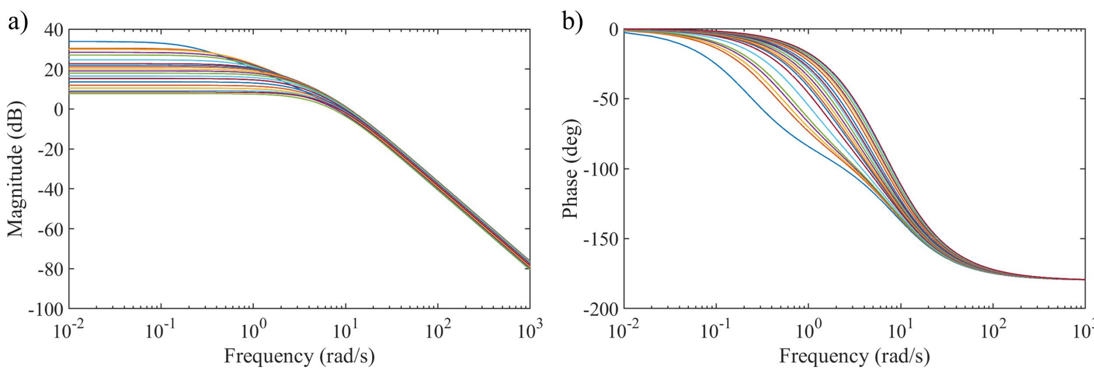

Fig. 6. Bode plot of the equivalent plants: a) magnitude, b) phase.

For controller synthesis, following weighting functions are selected:

$$W_1(s)=0.5\frac{s+a}{s+0.012},\ \ W_2(s)=b\frac{s+0.0001}{s+10}, \tag{12}$$

where a and b present coefficients which depend on intervals of relative shaft angular velocities. Obtained controllers are the 5th order controllers. By using the same procedure as for the fuel supply controller synthesis, they can be reduced to PI controllers. Coefficients a and b, full order controllers as well as PI controllers (proportional K_{p} and integral K_{i} gains) for each interval of shaft relative angular velocities are presented in Table 2. Comparisons of performances of the full order controller and the PI controller for the shaft relative angular velocity interval 0.25-0.275 are presented in Fig. 7. From Fig. 7 it can be concluded that the controller reduction has very little impact to performances.

$\overline{N}$	a	b	Full order controllers	K_p	K_i
0-0.05	0.2	1500	$\frac{0.07718s^4 + 2.241s^3 + 21.87s^2 + 73.26s + 14.9}{s^5 + 186.2s^4 + 3318s^3 + 1.639\cdot 10^4 s^2 + 7123s + 83.13}$	0.00511	0.00216
0.05-0.075	0.4	150	$\frac{0.331s^4 + 9.681s^3 + 95.77s^3 + 333.2s + 124.7}{s^5 + 128.4s^4 + 2315s^3 + 1.284\cdot 10^4 s^2 + 1.472\cdot 10^4 s + 174.8}$	0.01504	0.00856
0.075-0.1	0.5	100	$\frac{0.5285s^4 + 15.48s^3 + 153.8s^2 + 540.7s + 227.5}{s^5 + 136.5s^4 + 2525s^3 + 1.464\cdot 10^4 s^2 + 1.987\cdot 10^4 s + 236.4}$	0.0186	0.01155
0.1-0.125	0.6	100	$\frac{0.2549s^4 + 7.49s^3 + 74.77s^2 + 266.4s + 127.7}{s^5 + 68.97s^4 + 1126s^3 + 6225s^2 + 8404s + 99.95}$	0.02025	0.01534
0.125-0.15	0.6	50	$\frac{1.026s^4 + 30.2s^3 + 302.8s^2 + 1092s + 577}{s^5 + 144.3s^4 + 2772s^3 + 1.726\cdot 10^4 s^2 + 2.909\cdot 10^4 s + 346.6}$	0.02563	0.01998
0.15-0.175	0.8	25	$\frac{0.8208s^4 + 24.38s^3 + 248.3s^2 + 930.4s + 644.1}{s^5 + 73.67s^4 + 1319s^3 + 8640s^2 + 1.798\cdot 10^4 s + 214.5}$	0.03447	0.03603
0.175-0.2	1.2	12.5	$\frac{3.471s^4 + 104.2s^3 + 1082s^2 + 4241s + 3709}{s^5 + 131.2s^4 + 2806s^3 + 2.148\cdot 10^4 s^2 + 5.511\cdot 10^4 s + 658.2}$	0.05076	0.06762
0.2-0.225	1.4	5	$\frac{5.982s^4 + 180.9s^3 + 1902s^2 + 7665s + 7531}{s^5 + 119.5s^4 + 2850s^3 + 2.563\cdot 10^4 s^2 + 8.064\cdot 10^4 s + 964}$	0.06553	0.09375
0.225-0.25	1.5	5	$\frac{14.55s^4 + 441.7s^3 + 4676s^2 + 1.913\cdot 10^4 s + 1.987\cdot 10^4}{s^5 + 243s^4 + 6281s^3 + 5.794\cdot 10^4 s^2 + 1.837\cdot 10^5 s + 2196}$	0.07021	0.1086
0.25-0.275	1.7	5	$\frac{7.8s^4 + 238.1s^3 + 2545s^2 + 1.063\cdot 10^4 s + 1.186\cdot 10^4}{s^5 + 131.3s^4 + 3155s^3 + 2.82\cdot 10^4 s^2 + 8.824\cdot 10^4 s + 1055}$	0.07758	0.1349
0.275-0.3	1.9	5	$\frac{9.737s^4 + 299.1s^3 + 3230s^2 + 1.378\cdot 10^4 s + 1.643\cdot 10^4}{s^5 + 147.4s^4 + 3597s^3 + 3.237\cdot 10^4 s^2 + 1.011\cdot 10^5 s + 1209}$	0.08439	0.1631
0.3-0.325	2.2	5	$\frac{23.01s^4 + 712.3s^3 + 7794s^2 + 3.409\cdot 10^4 s + 4.376\cdot 10^4}{s^5 + 283.8s^4 + 7360s^3 + 6.747\cdot 10^4 s^2 + 2.12\cdot 10^5 s + 2534}$	0.09531	0.2072
0.325-0.35	2.5	5	$\frac{157.1s^4 + 4905s^3 + 5.442\cdot 10^4 s^2 + 2.445\cdot 10^5 s + 3.363\cdot 10^5}{s^5 + 1608s^4 + 4.377\cdot 10^4 s^3 + 4.059\cdot 10^5 s^2 + 1.277\cdot 10^6 s + 1.526\cdot 10^4}$	0.1079	0.2644
0.35-0.375	2.7	5	$\frac{18.67s^4 + 586.2s^3 + 6562s^2 + 2.996\cdot 10^4 s + 4.288\cdot 10^4}{s^5 + 198.4s^4 + 4949s^3 + 4.44\cdot 10^4 s^2 + 1.371\cdot 10^5 s + 1639}$	0.1174	0.314
0.375-0.4	3	4	$\frac{19.07s^4 + 604.5s^3 + 6869s^2 + 3.22\cdot 10^4 s + 4.893\cdot 10^4}{s^5 + 163.4s^4 + 4083s^3 + 3.733\cdot 10^4 s^2 + 1.181\cdot 10^5 s + 1412}$	0.1419	0.4158
0.4-0.425	3.6	4	$\frac{34.92s^4 + 1124s^3 + 1.306\cdot 10^4 s^2 + 6.361\cdot 10^4 s + 1.045\cdot 10^5}{s^5 + 243s^4 + 6340s^3 + 5.896\cdot 10^4 s^2 + 1.883\cdot 10^5 s + 2251}$	0.1642	0.5569
0.425-0.45	4	4	$\frac{58.34s^4 + 1914s^3 + 2.287\cdot 10^4 s^2 + 1.164\cdot 10^5 s + 2.069\cdot 10^5}{s^5 + 342.7s^4 + 9118s^3 + 8.51\cdot 10^4 s^2 + 2.714\cdot 10^5 s + 3244}$	0.1897	0.7654
0.45-0.475	4	2.5	$\frac{85.1s^4 + 2792s^3 + 3.336\cdot 10^4 s^2 + 1.697\cdot 10^5 s + 3.019\cdot 10^5}{s^5 + 371.7s^4 + 1.052\cdot 10^4 s^3 + 1.043\cdot 10^5 s^2 + 3.53\cdot 10^5 s + 4221}$	0.2283	0.8581
0.475-0.5	4.2	2	$\frac{80.29s^4 + 2669s^3 + 3.249\cdot 10^4 s^2 + 1.699\cdot 10^5 s + 3.162\cdot 10^5}{s^5 + 291.4s^4 + 8348s^3 + 8.46\cdot 10^4 s^2 + 2.924\cdot 10^5 s + 3497}$	0.2685	1.085
0.5-0.525	4.2	2	$\frac{98.37s^4 + 3312s^3 + 4.101\cdot 10^4 s^2 + 2.197\cdot 10^5 s + 4.242\cdot 10^5}{s^5 + 382.9s^4 + 1.166\cdot 10^4 s^3 + 1.236\cdot 10^5 s^2 + 4.431\cdot 10^5 s + 5299}$	0.2289	0.9607
0.525-0.5	4.6	2	$\frac{67.15s^4 + 2280s^3 + 2.856\cdot 10^4 s^2 + 1.554\cdot 10^5 s + 3.071\cdot 10^5}{s^5 + 252.6s^4 + 7490s^3 + 7.878\cdot 10^4 4s^2 + 2.814\cdot 10^5 s + 3366}$	0.247	1.095

Table 2. Weighting functions coefficients, full order and PI controllers for each interval of shaft relative angular velocities.

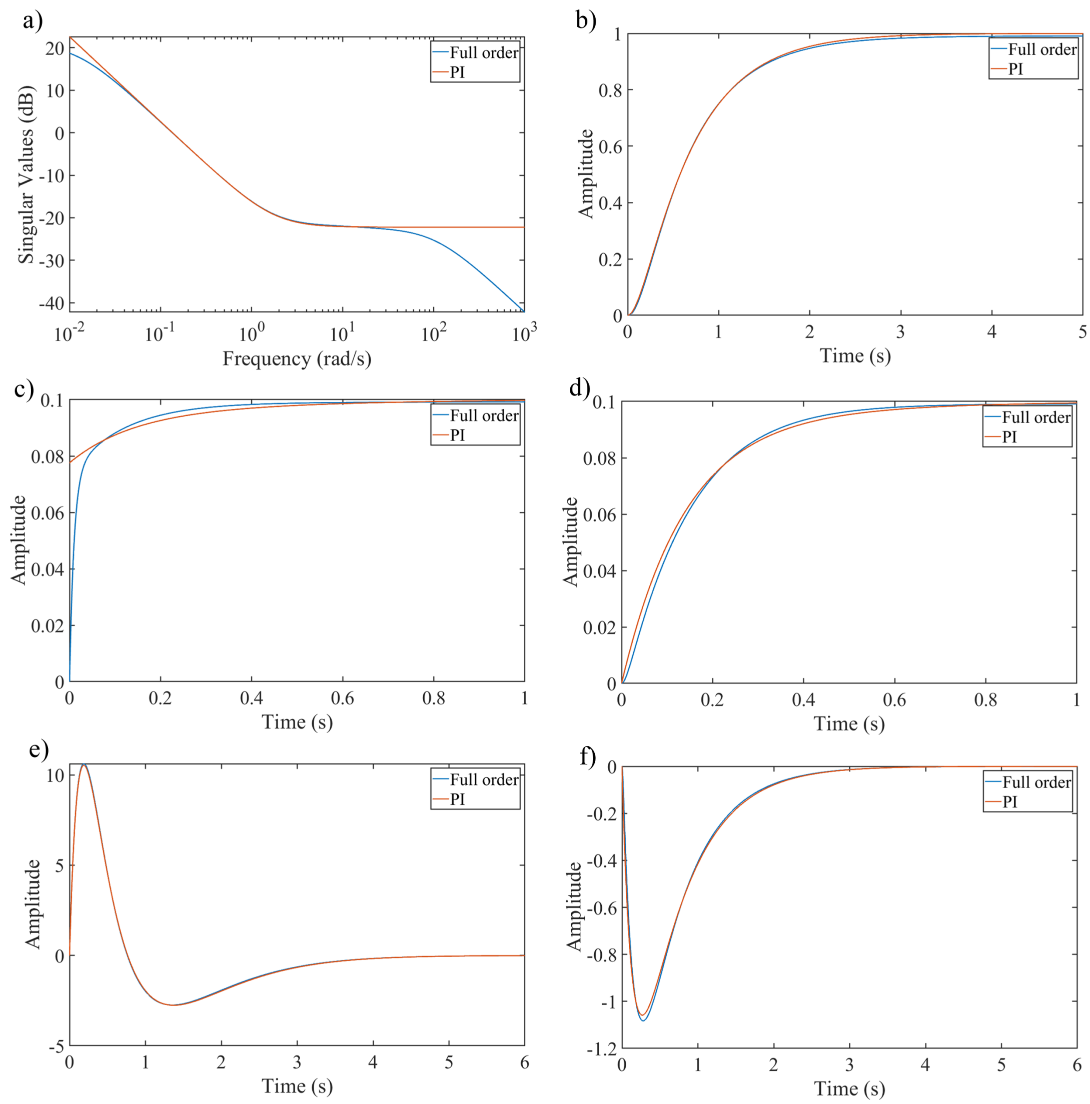

Fig. 7. Comparisons of performances of the full order and the PI controller for the shaft relative angular velocity interval 0.25-0.275: a) singular values, b) step response from the reference to the output, c) step response from the reference to the input to the fuel supply system, d) step response from the reference to the input to the engine (the fuel mass flow rate), e) impulse response from disturbance at the input to the output, f) impulse response from disturbance at the output to the output.

4. Simulation results

Obtained controller parameters are then combined via gain-scheduling approach and simulation is performed for following flight regime:

- 0 s-20 s: reference thrust is 2000N;
- 20 s-30 s: reference thrust is 4000N;
- 30 s: reference thrust is 600 N.

Simulation results are presented in Fig. 8. From Fig. 8 it can be concluded that all specifications are satisfied and the presented control algorithm shows good performances regarding the reference tracking.

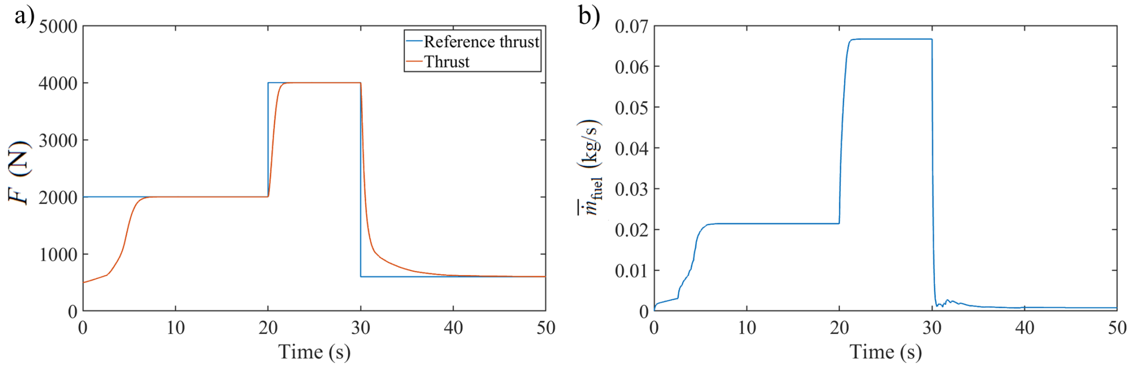

Fig. 8. Simulation results: a) obtained thrust compared to the reference thrust versus time, b) relative fuel mass flow rate versus time.

5. Conclusions

This paper presents the design of a thrust controller for a single-shaft turbofan engine at the operation point defined with following parameters: altitude = 0, Mach number = 0, angle of attack = 0. From nonlinear mathematical model of the engine, the 1st order transfer functions are obtained for selected shaft angular velocities. The fuel supply system is modeled by the 1st order transfer function. First, the fuel supply system controller is obtained by using the H_∞ methodology and it is reduced to the PI controller. After that, the fuel supply controllers for selected intervals of shaft angular velocities are obtained by using the H_∞ methodology and they are also reduced to PI controllers. Comparing performances of the full order controller and the PI controller it can be concluded that the order reduction has very little impact to performances. Obtained controller parameters are then combined via gain-scheduling approach. Simulation results show that all specifications are satisfied and the presented control algorithm shows good performances regarding the reference tracking.

Next stage is experimental identification of the fuel supply pump, implementation of obtained transfer function, application of presented procedure for controller synthesis and experimental validation on the test rig. After that, different altitudes, Mach numbers and angle of attack will be considered in order to obtain thrust controllers for whole operating envelope.

Acknowledgments

This work is supported by:

- Ministry of Science and Technological Development of Republic of Serbia through contract on realization and financing of scientific research work of accredited Serbian science and research organizations in 2021: 451-03-9/2021-14/200105

- Mechatronics Unmanned Systems & Technology Solutions d.o.o.

References

[1] Skogestad, S., Postlethwaite, I., *Multivariable Feedback Control: Analysis and Design, 2nd Edition,* John Wiley & Sons, Hoboken, NJ, 2005.

[2] Zhou, K., Doyle J.C, *Essentials of Robust Control*, Prentice-Hall, Englewood Cliffs, NJ, 1997.

[3] Gaudet, S.R., *Development of a Dynamic Modeling and Control System Design Methodology for Gas Turbines,* M.Sc. thesis, Carleton University, Ottawa, Ontario, 2007.

[4] Yazar, I., Kiyak, E., Caliskan, F., Karakoc, T.I., *Simulation-Based Dynamic Model and Speed Controller Design of a Small-Scale Turbojet Engine,* Aircraft Engineering and Aerospace Technology, Vol. 90, 351–358, 2018.

[5] Turns, S., *An Introduction to Combustion: Concepts and Applications, 2nd Edition,* McGraw-Hill Education, 2000.

[6] Zamani, M., Sadati, N., Ghartemani, M.K, *Design of an H_∞ PID Controller Using Particle Swarm Optimization*, International Journal of Control, Automation and Systems, Vol. 7, 273-280, 2009.

[7] Zorić, N., Radulović, R., Jazarević, V., Mitrović, Z., *Design of H_∞ Proportional-Integral Thrust Controller for Ramjet Engine,* Journal of Theoretical and Applied Mechanics, Vol. 58, 997-1007, 2020.

[8] Zorić, N., Radulović, R., Jazarević, V., Petrović, T., *H_∞ Robust Control of Ramjet Engine,* 9th International Scientific Conference on Defensive Technologies, OTEH 2020, Belgrade, Serbia, 15 – 16 October, 2020.